

OBSERVATIONS OF TOTAL INTERNAL REFLECTION AT A NATURAL SUPER-HYDROPHOBIC SURFACE

BY LORNE WHITEHEAD, MICHELE MOSSMAN AND ALEXANDRA KUSHNIR

The interaction of fluid drops on surfaces is an important and well-studied field involving energy associated with the interfaces between immiscible materials. This energy is usually called surface tension, is often represented with the symbol γ , and has units of N/m (a force per unit length), or equivalently, J/m² (an energy per unit area). It is well known that fluid interfaces tend to change shape to minimize their surface area and hence their surface energy [1]. In this paper, we will focus on a system that involves three distinct materials – water (in the form of a drop), a solid (forming an adjacent flat substrate), and air (surrounding both), as shown in Figure 1. In turn, there are three different surface tensions that determine the shape of the water drop – that of the surface-water interface (γ_{sw}), the water-air interface (γ_{wa}), and the surface-air interface (γ_{sa}).

If one ignores gravity, which is relatively unimportant for small drops, the shape of the surface depends entirely on the relative magnitudes of the surface tension values and

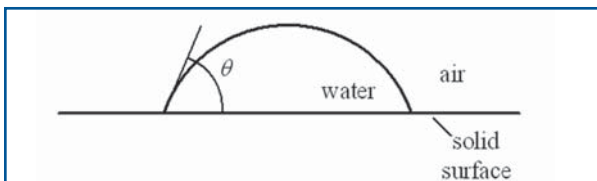


Fig. 1 Surface tension characteristics determining the shape of a water drop on a surface.

SUMMARY

It is well known that some plant leaves, most notably those of the lotus plant, possess super-hydrophobic properties as a self-cleaning feature as a result of the presence of microscopically small surface features. We have recently noted that the leaves of the arbutus tree exhibit similar properties, and that when the leaf is immersed in water, the air trapped within the nanostructures results in conditions that are favourable for total internal reflection (TIR), causing the leaf to appear extremely reflective from some viewing directions. In this paper, we discuss the basic optical principles behind this natural, unusual and visually interesting manifestation of the phenomenon of TIR.

is a portion of a sphere. That portion is typically described by specifying the so-called contact angle, θ , which is the angle the surface of the drop makes with the solid surface, measured from the inside of the drop. Young's Equation [2] in Equation (1) describes the relationship between the contact angle and the surface tension forces.

$$\cos \theta = \frac{\gamma_{sa} - \gamma_{sw}}{\gamma_{wa}} \quad (1)$$

A water drop on PTFE, as an example, typically has a contact angle of roughly 100° [3] and there is a wide range of values for other materials. Importantly, it is only the atoms and molecules at the solid surface that determine the contact angle, so very thin film coatings can profoundly alter the contact angle.

Such behaviour of drops on a surface is important in a wide range of circumstances. In some situations, for example in coating applications, it is important that the water has a very low contact angle so that it easily coats or “wets” the material. Surfaces that wet easily are often referred to as hydrophilic. In other cases, such as in waterproof clothing, it is desirable for water to “bead up”; the term hydrophobic is used to describe surfaces of this type that tend to repel water even in wet conditions.

For readily available materials, the contact angle on a smooth hydrophobic surface is generally less than about 120° [4]. However, the angle can be increased quite dramatically by using a rough or structured surface instead of a smooth one [5]. If the rough surface has the correct size and distribution of surface features, it can exhibit so-called super-hydrophobic properties by trapping air voids between the surface features [6]. This happens because the intrinsic surface properties of the material results in a contact angle between the water and the material that is sufficiently high that the water cannot flow into the interstitial regions to displace the air. The drop instead rests only on the hydrophobic tips of the features, and in order to minimize the total energy in the system, the drop assumes a much more complete spherical shape, with a contact angle greater than 150° [7], as shown in Figure 2.

The contact angle for a super-hydrophobic material has been estimated by various methods. A simple example is Wenzel's model [8] as shown in Equation (2) below.

$$\cos \theta_{\text{rough}} = r \cos \theta_{\text{smooth}} = r \frac{(\gamma_{sv} - \gamma_{sl})}{\gamma_{lv}} \quad (2)$$



Lorne Whitehead <lorne.whitehead@ubc.ca>, Michele Mossman and Alexandra Kushnir, Department of Physics and Astronomy, University of British Columbia, 6224 Agricultural Road, Vancouver, BC, V6T 1Z1



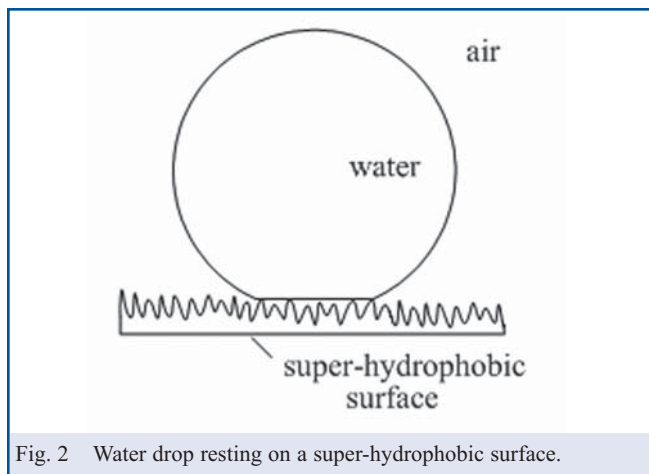


Fig. 2 Water drop resting on a super-hydrophobic surface.

This is a modified version of Young's equation, in which the roughness factor, r , is defined as the ratio of the total area of a rough surface to the effective surface area of the tips that is in contact with the water drop. This value of the surface area ratio is always greater than 1, so the contact angle for a rough surface will always be greater than that of a smooth surface.

In addition to having a myriad of practical applications in industry, hydrophilic, hydrophobic and super-hydrophobic materials also occur in some naturally-adapted forms. Perhaps the best known example is the leaf of the lotus plant, a type of water lily that is native to Asia. Scanning electron micrograph images have shown that surface of the lotus leaf has microscopically small bumps and tiny hair-like structures. Together with the naturally hydrophobic properties of the waxy leaf material, these nano-scale surface features give rise to a super-hydrophobic surface with a contact angle of greater than 150° [9].

It is thought that this surface evolved as a self-cleaning mechanism. The water drop actually makes very little contact with the highly convoluted surface, which means that raindrops roll down the leaf with very little friction. Along the way, the raindrop collects dirt and bacteria, thus cleaning the leaf. This explains how the lotus' leaves remain extremely clean, even though the water tends to be very dirty in their natural pond habitat. The existence of this natural phenomenon has fascinated scientists since it was first understood in 1975 [9,10] and it initiated an important branch of nanotechnology research [11-13].

THE STRUCTURE OF AN ARBUTUS LEAF

We have recently observed that the leaf of the arbutus tree exhibits a similar super-hydrophobic property. The arbutus tree, a photograph of which appears in Figure 3, is a broadleaf evergreen tree with unusually smooth, orange bark and red berries. It grows in a very limited area in North America, in small comparatively dryer pockets near the sea, between southern British Columbia and the northern California.

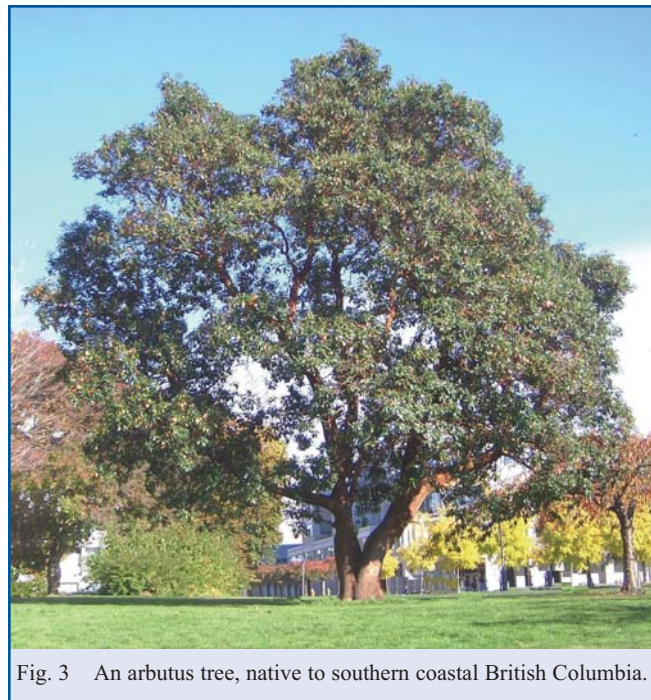


Fig. 3 An arbutus tree, native to southern coastal British Columbia.

Interestingly, in the case of the arbutus leaf, it is only the underside of the leaf that exhibits the super-hydrophobic property. One might wonder what the evolutionary advantage of such an arrangement may have been. Since the stomata (the gas transport pores in the leaf) are on the underside, perhaps there may have been an advantage in keeping them free of a water film in order to maintain air flow. Given the relatively pristine environment in which the tree grows, maintaining a clean top surface may not have been problematic, and the small benefit of a hydrophobic leaf top surface may have been outweighed by the metabolic cost of such a coating and/or a resultant reduction in light transmission – a problem that would be more significant in a northern climate.

At any rate, we have examined the surface structure and have confirmed that it has hair-like features with a diameter of about 100 nm and spacing of about 1000 nm as shown in the scanning electron micrograph in Figure 4.

We cannot accurately determine the roughness factor, r , from such an image. However, it appears to lie approximately in the range from 3 to 5. If the materials from which the hairs form have a mildly hydrophobic contact angle of about 100° , then the application of Wenzel's law would yield a net contact angle in the range 120° to 150° . We placed a 2 mm diameter water drop on the surface of the leaf, as shown in Figure 5, and observed a contact angle of approximately 140° , consistent with the SEM observations and such considerations.

The existence of this super-hydrophobic property on the arbutus tree is not in itself scientifically noteworthy (although as mentioned above it is interesting that it is restricted to the leaf underside). Rather, it is the combination of this natural super-



S4700 1.5kV 5.2mm x5.00k SE(U) 9/18/07 10.0um
 Fig. 4 Scanning electron micrograph of the underside of an arbutus leaf.

hydrophobicity with another well-known, but unrelated, phenomenon in physics, total internal reflection, which we present here as an interesting demonstration of physics in nature.

TOTAL INTERNAL REFLECTION AT A SUPER-HYDROPHOBIC INTERFACE

Total internal reflection (TIR) is an optical phenomenon that can occur when a light ray traveling in a transparent material with index of refraction n_i encounters an interface with a material having a lower index of refraction, n_t . The occurrence of TIR depends on the angle of incidence and the ratio of the refractive index values of the two materials. This ratio determines a critical angle, θ_c , for the interface, as shown in Equation (3):

$$\theta_c = \sin^{-1}\left(\frac{n_t}{n_i}\right) \quad (3)$$

By convention, angles of incidence are measured from a reference direction perpendicular to the surface in question. If this value is less than the critical value, the light will partially reflect and partially transmit into the second material, but for

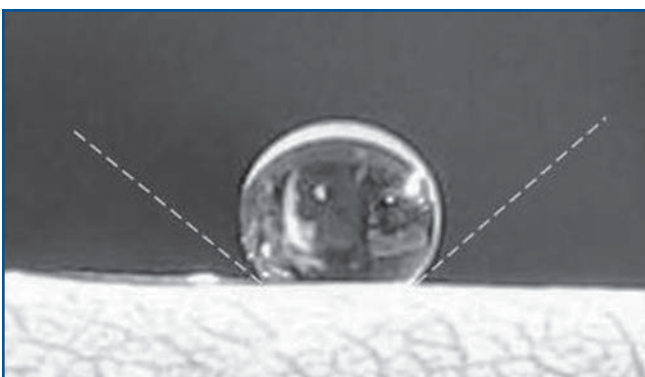


Fig. 5 A water drop on an arbutus leaf exhibits a contact angle of 140°.

all angles of incidence greater than the critical angle, the light will be completely reflected by means of TIR. As an example, the critical angle for a water/air interface where $n_i = 1.334$ and $n_t = 1.000$ is 48.8°.

When TIR is occurring, there is no net transfer of electromagnetic energy across the interface, but the complete solution of the Maxwell equations shows that a small amount of the electromagnetic field energy actually penetrates a small distance into the second material. This phenomenon, referred to as an evanescent wave, corresponds to a propagation of energy along the interface with an intensity that decreases exponentially as a function of depth into the second material. The mean penetration depth is usually less than a half wavelength, which for visible light is about 250 nm. This concept is depicted schematically in Figure 6.

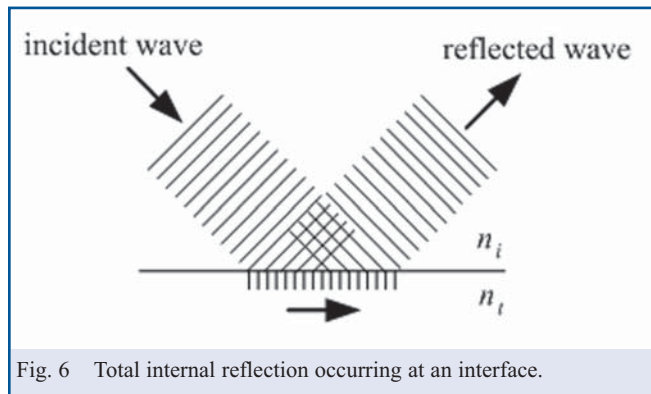


Fig. 6 Total internal reflection occurring at an interface.

It is also well known that TIR can be prevented, or “frustrated”, by absorbing the energy in the evanescent wave, which can be done by moving an absorptive or optically dense material into the region near the interface that is occupied by the evanescent wave. For practical purposes, this means that as long as the second lower index material extends a distance equivalent to several penetration depths of the evanescent wave, TIR will efficiently occur. Interestingly, because of the small thickness of the evanescent wave, this means the required thickness is about 1 or 2 μm .

TIR has been well-studied and is useful in a number of important applications, perhaps the most notable being the propagation of electromagnetic waves in fibre optic communication systems. Moreover, although it is rare, the phenomenon of TIR can occasionally be viewed in nature, for example in a mirage^[14], and recently we have observed that a water-immersed arbutus leaf provides another such natural occurrence.

Considering again the micrograph image in Figure 4, it appears that at least 90% of the volume in the structured surface region is comprised of air, and that therefore the effective refractive index of this region should be close to 1.0, perhaps approximately 1.05. This region is several micrometers thick and therefore ought to be sufficient to cause total internal reflection

when immersed in water, given that this index value is much less than the value of 1.334 for that liquid. Furthermore, the super-hydrophobic nature of the surface should ensure that a low index value is maintained in the presence of water, as it would be energetically unfavourable for water to fill the nano-scale voids.

Such expectations are indeed realized when the leaf is viewed underwater, as shown in Figure 7. For small angles of incidence, the leaf looks like a leaf; for large angles of incidence the leaf looks like a piece of silver; and at approximately the anticipated critical angle, the angular variations within the leaf cause a mixed appearance.



Fig. 7 Photograph of TIR occurring on the underside of an arbutus leaf.

While the reflection shown in Figure 7 is remarkably long-lived under ordinary conditions, we were able to show that it could be easily destroyed in two ways, both of which remove the air. The first way was to add detergent to the water, lowering the surface tension of the air-water interface. In this case, the observed TIR appearance vanished within seconds. The second way was to submerge the leaf in de-aired water, (prepared by vigorously boiling the water and then cooling it in a sealed container). In this case, the leaf at first appears highly reflective as in Figure 7, but over a few minutes the TIR appearance fades away, presumably as the air dissolves into the water.

It should also be noted that super-hydrophobic leaves are not the only immersed super-hydrophobic surfaces capable of appearing highly reflective. We have observed that a commercially available spray-on super-hydrophobic coating^[15] has a similar effect. And considering again naturally occurring systems, there have been anecdotal reports of the “silvery” appearance of the plastrons of certain insects underwater^[16,17], an effect that is presumably caused by a similar phenomenon. At any rate, the comparatively flat underside of the arbutus leaf has provided an opportunity whereby this naturally-observed effect can be measured in order to establish that TIR is indeed taking place.

QUANTIFYING THE REFLECTION CHARACTERISTICS

In order to establish that the observed reflectance is caused by TIR, we have measured it by comparing the surface luminance to that of a specular metallic surface of known reflectance R_s (aluminized polyester film, $R_s \approx 85\%$). The leaf was immersed in water in a transparent tank within a diffusely reflective 1 m diameter integrating sphere illuminated uniformly by a 50 W 3000 K quartz-halogen incandescent lamp powered by a regulated DC supply. Front surface reflection from the tank was minimized by carefully aiming the reflected view from that surface toward a small black patch. We used a photometric luminance meter to measure the luminance of an 8 mm circular region on the leaf and that of the immediately adjacent coplanar specular reference surface, over a 60° angular range spanning the anticipated critical angle, which for an interface between pure water and a mixture of 10% polymer (with index about 1.5) and 90% air (with index of 1.0) would be about 52° .

Figure 8 shows that when the leaf is immersed in water, as compared to when it is immersed in air, the reflectance does rapidly increase to a high value that is close to 100% as the viewing angle moves through the region near the anticipated critical angle.

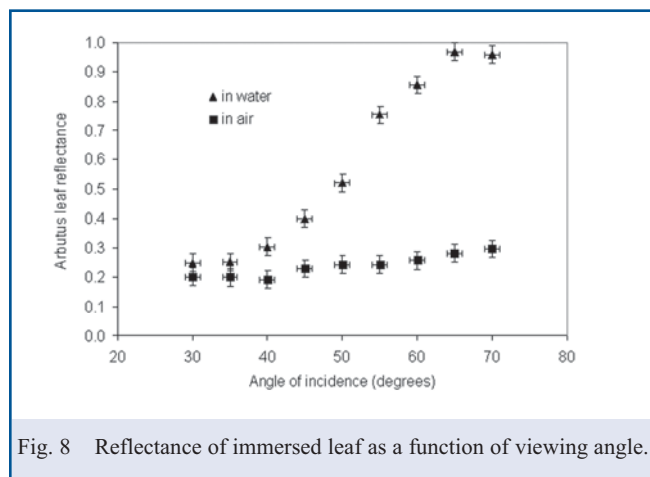


Fig. 8 Reflectance of immersed leaf as a function of viewing angle.

It is interesting to consider how the reflectance measurements carried out in air relate to those done in water. In both cases, we believe the reflective surface of the leaf is in contact with the super-hydrophobic layer, which is mainly air, and this leaf reflectance, which we can label R_{la} should therefore be the same. The difference caused by measuring under water is simply the addition of one optical interface – that between the water and the super-hydrophobic layer, whose reflectance can be labeled R_{aw} . When two reflective surfaces are adjacent to one another, and incoherent light is employed, the combined reflectance R is easily determined by calculating the rapidly converging sum of the infinite series of inter-reflections. It is thus straightforward to show that these reflectance values are related as shown in Equation (3):

$$R = R_{aw} + \frac{R_{ia}(1 - R_{aw})^2}{1 - R_{ia}R_{aw}} \quad (3)$$

By inverting this relation we obtained the values of R_{aw} that would be required to yield the observed values of R and R_{ia} of Figure 8. These measurement-derived R_{aw} values are plotted in Figure 9.

We can now consider whether these values for R_{aw} are those that would be expected for such an interface. To check this, we calculated the anticipated reflectance for non-polarized incoherent light using the Fresnel equations as shown in Equation 4:

$$R = \frac{1}{2} \left(\frac{\sin^2(\theta_t - \theta_i)}{\sin^2(\theta_t + \theta_i)} + \frac{\tan^2(\theta_t - \theta_i)}{\tan^2(\theta_t + \theta_i)} \right) \quad (4)$$

where θ_t is determined from Snell's law, $\theta_t = \sin^{-1}((n_i/n_t)\sin(\theta_i))$, and θ_i and θ_t are, respectively, the incident and transmitted angle. For n_i we used the known value for the refractive index of water, 1.334, and for n_t we used an estimated value of 1.05 for the effective refractive index of the super-hydrophobic fibre/air layer. To take into account the slightly non-planar nature of the leaf surface we convoluted the result with a Gaussian angular distribution, finding that adjusting the standard deviation to a reasonable value of 8° gave the best fit. (This value was confirmed to be reasonable by directing a laser beam, with an angle of incidence greater than θ_c , at the surface of the leaf and observing the angular spread of the reflected light.) As shown in Figure 9, these calculated values agree reasonably well with those derived from the measurements in Figure 8.

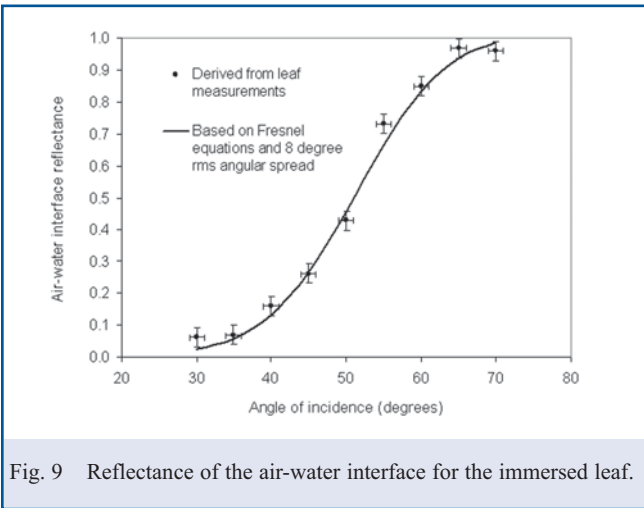


Fig. 9 Reflectance of the air-water interface for the immersed leaf.

These observations leave little doubt that the observed reflectance is indeed the result of total internal reflection at the boundary between the water and the air-filled super-hydrophobic layer.

DISCUSSION

The measurement of total internal reflection on the surface of an arbutus leaf has enabled a quantitative evaluation of an effect that has been observed in several other naturally-occurring super-hydrophobic systems. When the super-hydrophobic properties of the lotus leaf first were first understood, a wide range of biomimetic research ensued, including development of new non-wetting and self-cleaning materials. Similarly, although the work reported here focuses on a natural phenomenon and not on any specific application, it has nonetheless stimulated our interest in possible optical uses of super-hydrophobic layers. In particular, it is interesting to consider means of controlling the degree of reflection of a super-hydrophobic surface. Such controlled reflection could be useful in a number of areas, including optical switches, beam steering systems and electronic image displays.

CONCLUSION

To the best of our knowledge this paper represents the first quantitative verification of total internal reflection in underwater air-filled super-hydrophobic nano-structured films, but the advancement of scientific knowledge is not the primary goal of this paper. Rather, our view is that arbutus leaves serve as an interesting natural manifestation of a phenomenon that might otherwise have only been observed through experimentation in a research laboratory. Just as a rainbow tells us little new about refraction, dispersion or diffraction, these arbutus leaf observations have not advanced our understanding of total internal reflection. However, it is worthwhile (and non-trivial) to understand a rainbow, and similarly, we hope the work described here may advance in a small way our appreciation of nature and the remarkable complexities of evolved nanostructures that employ subtle physical laws and are essential to all forms of life.

ACKNOWLEDGEMENTS

The authors thank the Natural Sciences and Engineering Research Council of Canada and 3M Company for their support of this work. The authors are also grateful to Dr. Peter Hrudevy for his contributions to this paper.

REFERENCES

1. F. White, *Fluid Mechanics*, McGraw-Hill, New York, p. 30, 1986.
2. T. Young, "An essay on the cohesion of fluids", *Philos. Trans. R. Soc.*, **95**, 65-87 (1805).
3. T. Yasuda, T. Okuno and H. Yasuda, "Contact Angle of Water on Polymer Surfaces," *Langmuir*, **10**, 2435-2439 (1994).
4. T. Nishino, M. Meguro, N. Katsuhiko, M. Matsushita, and Y. Ueda, "The lowest surface free energy based on CF₃ alignment," *Langmuir*, **15**, 4321-4323 (1999).
5. A. Cassie and S. Baxter, "Wettability of porous surfaces", *Trans. Faraday Soc.*, **40**, 546-551 (1944).
6. S. Herminghaus, "Roughness-induced non-wetting", *Europhys. Lett.*, **52**, 165-170 (2000).
7. A. Nakajima, H. Kazuhito, and T. Watanabe, "Recent studies on super-hydrophobic films", *Monatsh. Chem.*, **132**, 31-41 (2001).
8. R. Wenzel, *Ind. Eng. Chem.*, **28**, 988 (1936).
9. C. Neinhuis and W. Barthlott, "Characterization and distribution of water-repellent, self-cleaning plant surfaces", *Ann. Bot.*, **79**, 667-677 (1997).
10. W. Barthlott and C. Neinhuis, "Purity of the sacred lotus, or escape from contamination in biological surfaces", *Planta*, **202**, 1-8 (1997).
11. H. Erbil, A. Demirel, Y. Avci and O. Mert, "Transformation of a simple plastic into a super-hydrophobic surface", *Science*, **299**, 1377-1380 (2003).
12. D. Quere, A. Lafuma and J. Bico, "Slippy and sticky microtextured solids", *Nanotechnology*, **14**, 1109-1112 (2003).
13. N. Shirtcliffe, G. McHale, M. Newton, C. Perry and B. Pyatt, "Plastron properties of a super-hydrophobic surface", *Appl. Phys. Lett.*, **89**, 104106 (2006).
14. L. Whitehead, M. Mossman, and A. Kotlicki, "Visual applications of total internal reflection in prismatic microstructures", *Physics in Canada*, **57**, 329-335 (2001).
15. HIREC 100™, NTT Advanced Technology Corporation, Shinjuku Mitsui Building 2-1-1, Nishi-shinjuku, Shinjuku-ku, Tokyo 163-0431, Japan.
16. W. Lee, M.K. Jin, W.C. Yoo and J.K. Lee, "Nanostructuring of a polymeric substrate with well-defined nanometer-scale topography and tailored surface wettability", *Langmuir*, **20**, 7665-7669 (2004).
17. X. Gao and L. Jiang, "Water-repellent legs of water striders", *Nature*, **432**, 36 (2004).